Journal of Drug Delivery Science and Technology 61 (2021) 102149

Contents lists available at ScienceDirect

Journal of Drug Delivery Science and Technology

journal homepage: www.elsevier.com/locate/jddst

Research paper

Design and manufacturing of monodisperse and malleable phytantriol-based cubosomes for drug delivery applications

Barbara Malheiros [a], Raphael Dias de Castro [a,b], Mayra C.G. Lotierzo [a], Bruna R. Casadei [b], Leandro R.S. Barbosa [b,*]

[a] Department of Biochemical and Pharmaceutical Technology, University of Sao Paulo, Av Prof Lineu Prestes 580 Bloco 16, BR-05508000, São Paulo, SP, Brazil
[b] University of São Paulo, Physics Institute, Rua Do Matão, 1371, 05508-090, São Paulo, SP, Brazil

ARTICLE INFO

Keywords:
Cubosomes
Extrusion
Lyophilization
Malleability
SAXS
NTA
Phytantriol

ABSTRACT

In this study, we report the detailed characterization of phytantriol-based cubosomes submitted to stressing processes, such as lyophilization and extrusion. Lyophilization (or freeze-drying) of nanoparticles systems can be challenging with respect to preserving physicochemical properties and the biological activities of the materials. Extrusion can be used to prevent agglutination, sedimentation and Ostwald ripening or droplet coalescence, resulting in homogeneous size distribution of the formulation and smaller particle size. Samples in both ultra pure water and PBS buffer were analyzed by SAXS, DLS, NTA and electron microscopy. It was found that cubosomes hold their morphological features when lyophilized with a minor change in particle size, a decrease of 3.5% in ultra pure water and an increase of 16% in PBS buffer, as well as an increase in particle polydispersion. Regarding nanoparticle concentration, there is a considerable decrease from 4.09± 0.66 x 10^{12} particles/mL to 1.76± 0.66 x 10^{12} particles/mL in ultrapure water and from 6.67± 0.84 x 10^{12} particles/mL to 1.43± 0.34 x 10^{12} particles/mL in PBS buffer. When extruded, the cubic structure is preserved. Curiously, particle size is not affected by the pore size of the extrusion filter, as compared to liposomes, for instance. On this ground, cubosomes show great malleability even when undergoing extrusion in a 50 nm pore size filter, presenting average size of 185± 2 nm compared to 237± 5 nm of the control sample in ultra pure water and 277± 3 nm compared to 229± 1 nm in PBS buffer. Polydispersion is not affected by this process. Regarding concentration, for both systems, there is an increase from 4.09± 0.66 x 10^{12} particles/mL to 7.88± 0.66 x 10^{12} particles/mL in ultra pure water and from 6.67± 0.84 x 10^{12} particles/mL to 8.54± 0.15 x 10^{12} particles/mL in PBS buffer, indicating that larger particles are broken into smaller ones, in a rearranging process. Finally, it was shown that cubosomes are very malleable once they can undergo stressing processes without alterations in particle size or morphology. We believe that these results can improve our understanding of the cubosome structure, and can even bring new possibilities of applications due to its high malleability.

1. Introduction

In the last decades, non-lamellar nanoparticles have gained a lot of attention due to its versatility and capabilities [1–3]. This is due mainly to its high surface area > 400 m^2 g^{-1} and cubic structure [4,5]. In addition, it has the ability to incorporate either hydrophobic, hydrophilic or amphiphilic molecules [3,6,7]. Noteworthy, generally more then 50 % of the cubosome inner volume is hydrophobic, making it an interesting system for very hydrophobic drugs carrier [8].

Cubosomes are three-dimensional nanoparticles mainly found in three different cubic structures: *Ia3d*, *Pn3m* and *Im3m* [9,10]. Some lipids (mainly monoglycerides, glycolipids and phytantriol, Fig. 1A) show polymorphism in which the cubic phases are present in a great area of their phase diagram, in excess of water [9,11,12]. These cubic phases are regarded as the most complex structures in liquid crystalline systems, being first characterized by Luzzati pioneering studies in the 60's [13]. Cubosomes can be produced by breaking the reverse bulk cubic phases, resulting in a colloidal suspension [14,15], in the presence of an non-ionic polymer, for steric stabilization, like Poloxamer F127 (Fig. 1B).

Phytantriol (PHY, Fig. 1A) has been studied for cubosome production for the last two decades [16–18]. PHY is biocompatible, has cosmetic applications and displays cubic *Pn3m* self-assembled structure in excess

* Corresponding author.
E-mail address: lbarbosa@if.usp.br (L.R.S. Barbosa).

https://doi.org/10.1016/j.jddst.2020.102149
Received 14 August 2020; Received in revised form 22 September 2020; Accepted 8 October 2020
Available online 16 October 2020

Abbreviations

Cryo-EM	cryogenic electron microscopy
D_H	hydrodynamic diameter
DLS	dynamic light scattering
F127	pluronic F-127
FFT	Fast Fourier Transform
NTA	nanoparticle tracking analysis
PHY	phytantriol
PHY-cub	phytantriol based cubosomes
SAXS	small angle X-ray scattering

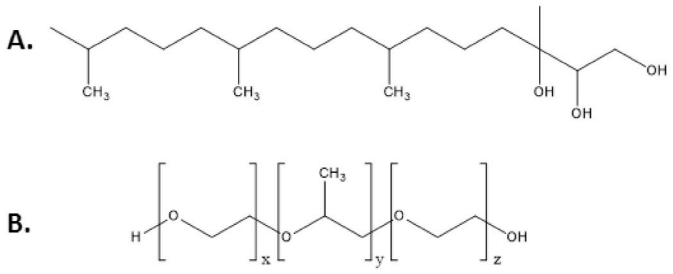

Fig. 1. Chemical structure of phytantriol (A) and Pluronic F127 (B). In Fig. 1B, x and y are 100 and 65, respectively.

of water [12,19]. PHY became an interesting molecule for drug delivery nanoparticles production because it does not have any insaturation in the alkyl chain, as monoolein (glycerol monooleate). The absence of an ester bond in the polar head group (like monoolein, for instance) also makes PHY less susceptible to chemical degradation by the gastrointestinal tract (acidic pH) [18,20,21].

Typically, cubosome nanoparticles are formulated in solution as colloidal systems, and cannot be stored for long periods due to physical (aggregation) and chemical instability [17,22]. Thus, it is important to study some other conditions where the PHY cubosomes could be stored for longer periods to increase its shelf life. There are some process used in pharmaceutical industries to increase the stability of some specific formulation. For instance, lyophilization (or freeze-drying) is of great interest due to its potential to provide longer shelf lives to pharmaceutical products [23–25]. Besides lyophilization, another process that can increase nanoparticle stabilization is extrusion. For instance, extrusion is widely used in large unilamellar vesicles (LUVs) preparation [26–28]. This process is generally used to guarantee a smaller polydispersity and controlled sized in vesicles, as well as to increase colloidal stability [29,30]. In addition, it can be used to prevent agglutination, sedimentation and Ostwald ripening (droplet coalescence), resulting in homogeneous size distribution of the formulation and smaller particle size, favoring their future pharmaceutical applications [31].

There is lack of detailed evidence regarding the behavior of cubosomes under both lyophilization and extrusion processes. Lyophilization has been explored by Shi et al. to investigate eventual changes in cubosome inner cubic symmetry due to this process [15]. According to the authors, the inner Pn3m cubic structure remained unaltered after lyophilization, but no details were given regarding the conditions of the morphological system. Regarding extrusion, Nilsson et al. produced radiolabeled cubosomes for theragnostic purpose using extrusion as a way of controlling particle size [32]. According to the authors, the extrusion using polycarbonate membranes with controlled pores of 100–800 nm was employed to ensure a narrow nanoparticle size distribution, again no details were provided regarding stability and morphology.

In the present study, we produced and systematically characterized phytantriol based cubosomes (PHY-cubs) in terms of structure, morphology, particle size and concentration under stressing processes, namely lyophilization and extrusion. In order to investigate if these processes could affect the phase behavior, we employed small angle x-ray scattering (SAXS), cryogenic transmission electron microscopy (cryo-TEM), dynamic light scattering (DLS) and nanoparticle tracking analysis (NTA). In addition, two different aqueous media (ultrapure waterand PBS buffer) were studied in order to see if the salts influence the cubosomal structure under such stressing processes.

2. Materials and methods

2.1. Materials

Phytantriol, 3,7,11,15-Tetramethylhexadecane-1,2,3-triol (PHY) with purity over 99 % was purchased from Avanti Polar Lipids Inc. Pluronic F127 (F127, poloxamer 407) with 99 % purity was purchased from Sigma-Aldrich/Merk®. Both were used as received. Ultrapure Milli-Q water was also used in the preparations.

2.2. Cubosomes preparation

Cubosomes colloidal dispersion was prepared based on a bottom up methodology [33]. Briefly, two solutions were made: one with 100 mg of PHY solubilized into 10 mL of ethanol. The second, where 25 mg of F127 was solubilized in 22.5 mL of ultrapure water or PBS buffer (10 mM phosphate monobasic, 2.7 mM KCl, 137 mM NaCl, pH 7.4). Subsequently, the PHY solution was dropwised into the F127 solution, at 45 °C under a magnetic stirrer and left to homogenize for 15 min. The final solution (33 mL) was brought to a rotary evaporator until a final volume of 5 mL. Samples were stored into glass vials and at room temperature. For lyophilization, samples were freezed at −80 °C overnight, and the evaporation process was performed in a Liotop® L101 lyophilizer at −53 °C for 22 h in low pressure (0.120 mbar). Extrusion was performed in a mini extruder from Avanti Polar Lipids Inc, with a home-made automatic device and a Peltier-based temperature control (45 °C), using low lipid binding polycarbonate membranes of 400, 200, 100, 50 and 30 nm pore sizes.

2.3. Small angle X-ray scattering (SAXS)

Experiments were performed in a synchrotron accelerator at the National Laboratory of Synchrotron Light (LNLS), Campinas, São Paulo, at the SAXS-1 beamline. Samples were inserted into a mica sample holder (1 mm thick) where 300 μ L of each sample was measured for 100 s. The used detector was a Pilatus 300K distant by $\sim 1m$ from the samples. For the diffraction peak analysis, an inhouse program was developed and used [29]. Briefly, a routine for peak recognition was employed in the web-based platform, the centered positions were calculated and the peak ratios were used to index the crystallographic space group of the samples. A calculation of the lattice parameter and water channel diameter was performed afterwards using the SCryPTA software [34].

2.4. Dynamic light scattering (DLS)

Dynamic Light Scattering measurements was applied to obtain the cubosome average size before and after lyophilization and extrusion, using the apparent translational diffusion coefficient, $D_t^0(c)$, at dilution conditions, i.e., $c \rightarrow 0$. DLS was performed in a ZetaSizer ZS90 equipment (Malvern, UK) using the detector positioned at 90° and a He–Ne laser, $\lambda = 632.8$ nm as a light source, being λ the radiation wavelength. All measurements were performed at 25 °C. Samples were diluted 20-fold or more to ensure no multiple scattering inside the cuvette during the DLS experiments. The results show a unimodal distribution and represent the

average of three measurements, data is the result of duplicate measurements. The apparent values of hydrodynamic diameter, which is related to the diffusional dynamics of a vesicle, were obtained with the time correlation functions and were analyzed by the cumulant analysis, using the software provided by Malvern. The hydrodynamic diameter (D_H)) determination was calculated by means of Stokes–Einstein equation, as follows:

$$D_H = \frac{k_B T}{3\pi\eta D_t^0(c)} \quad (1)$$

where k_B is the Boltzmann constant, T is the absolute temperature, η is the viscosity of the solvent and $D_t^0(c)$ is the translational diffusion coefficient and *c* the nanoparticle concentration.

2.5. Nanoparticle tracking analysis (NTA)

A nanoSight NS300 (Malvern Instruments) equipped with a green (532 nm) laser and a sample chamber (manual pumping) was used. Samples were diluted 7500x and measured in duplicate at room temperature (25 °C). Motion of particles was recorded with a CCD camera (screen gain 2, camera level 9, variable autofocus) and analyzed with the software (NTA version 3.2 Dev Build 3.2.16). From the frames taken, the motion of particles was analyzed with variable threshold, always maintaining between 50 and 70 particles per frame. Then, averaged diameter and standard deviation of the measurements were used to estimate particle mean size and total particle concentration of the samples. The curves of size distribution were also analyzed in order to evaluate size populations in the measurements.

2.6. Electron microscopy and data analysis

Transmission electron microscopy (TEM) experiments were performed in a FEI Tecnai G^2 F20 at 200 kV with a CCD camera Eagle 4 k HS. 5 μ L of sample was drop casted on 200 mesh formvar-carbon grids (Electron Microscopy Sciences®) submitted to a glow discharge procedure (14 mA, 20 s). Samples were stained with 5 μ L phosphotungstic acid at 2 % w/v for 30 s. Cryogenic electron microscopy (Cryo-EM) measurements were performed in a JEM-2100 JEOL microscope at 120 kV with a CMOS camera OneView 4kx4k. A 300 mesh Holey Lacey Carbon from Ted Pella® was used, grids were submitted to a glow discharge procedure (15 mA, 10 s) prior to the drop casting of the sample. In a Vitrobot® 3 μ L of sample was drop casted to the grid, giving 20 s for sample fixation. An automatic blotting was performed to dry the excess of sample with a negative blotting force. Subsequently, the grid was rapidly plunged into liquid ethane wrapped into a liquid nitrogen environment. Finally, grids were transposed to a grid box in liquid nitrogen until measurements. ImageJ® software was used to image analysis of TEM and Cryo-EM micrographs, sizes were evaluated and the internal structure of the nanoparticles could be assessed and analyzed by means of the fast Fourier transformation (FFT).

3. Results and discussion

3.1. Lyophilization affects particle concentration

In order to check for nanoparticles stability and conservation, phytantriol based cubosomes (PHY-cubs) were prepared in two different systems (ultrapure water or PBS buffer), submitted to lyophilization and then rehydration. Fig. 2 shows the SAXS curves of PHY-Cub before the lyophilization process (*control*, red curves) and after rehydrating the lyophilized samples (*lyophilized*, blue curves), in both systems: ultrapure water (*H_2O,* Fig. 2A) and PBS buffer (*PBS,* Fig. 2B).

Before the lyophilization process (*control*), both systems were characterized as *Pn3m* (or Q224) inner structure, with peak positions at: $\sqrt{2}$, $\sqrt{3}, \sqrt{4}, \sqrt{6}, \sqrt{8}, \sqrt{9}$ for the reflection relative to the planes: (110), (111), (200), (211), (220), (221), respectively, in good agreement with previous studies in literature [9,33,35,36]. The calculated unit cell parameters were 6.82 ± 0.03 nm and 6.76 ± 0.03 nm for systems in ultrapure water and PBS buffer, respectively, as shown in Table 1. All calculations were performed using SCryPTA in-house software [34].

After rehydration of the lyophilized cubosomes, in both studied systems, one can notice that the cubic symmetry (Pn3m) of the nanoparticles was not altered by the process. Interestingly, a shift to smaller q values can be noticed in the system in ultrapure water (Fig. 2A). Indeed, the observed cell parameters were 7.04 ± 0.05 nm (an increase of 3%) and 6.87 ± 0.04 nm (an increase of 1.6%) for the systems in the ultrapure water and PBS buffer, respectively. This fact indicates that in PBS buffer, the unit cell parameter was kept mainly unaltered, whereas it increased slightly in the system in ultrapure water. Moreover, using information about the surface of the lipidic bilayer of the cubosomes, it was possible to estimated the diameter of water channel. As in the case of lattice parameter, minor changes were evidenced before and after lyophilization, see Table 1. In ultrapure water the size of the water

Table 1
Calculated values of lattice parameter and water channel diameter from the Scrypta software for all samples: PHY-Cub before undergoing any processes (*control*) and after being lyophilized (*lyophilized*) or extruded (extruded 0.1 μm or 0.05μm) in both systems: ultrapure water (*H_2O*) and PBS buffer.

	lattice parameter (nm)	water channel diameter (nm)
Ultrapure water		
Control	6.82 ± 0.03	2.511 ± 0.012
Lyophilized	7.04 ± 0.05	2.590 ± 0.020
extruded 100 nm	6.86 ± 0.03	2.524 ± 0.013
extruded 50 nm	6.89 ± 0.04	2.635 ± 0.015
PBS buffer		
control	6.76 ± 0.03	2.488 ± 0.012
lyophilized	6.87 ± 0.04	2.530 ± 0.013
extruded 100 nm	6.79 ± 0.04	2.498 ± 0.013
extruded 50 nm	6.80 ± 0.04	2.503 ± 0.015

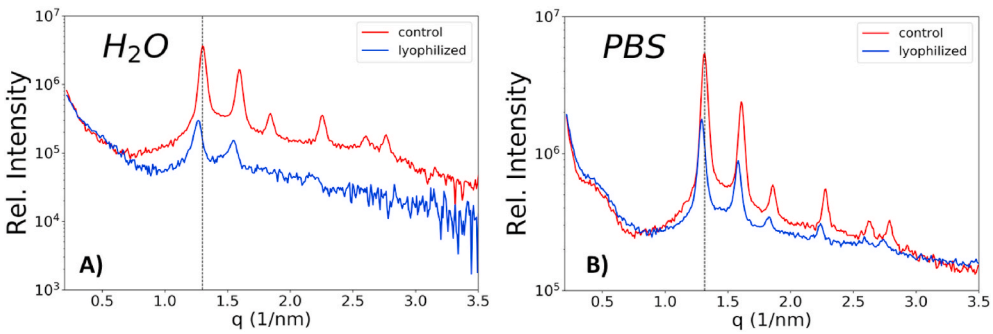

Fig. 2. SAXS curves of PHY-Cub in the ultrapure water (*H_2O*, A) and PBS buffer (*PBS*, B), before (*control*, red curves) and after lyophilization process (*lyophilized*, blue curves). After rehydration of the lyophilized sample, in water medium only two diffraction peaks are visible (blue line - Fig. 2-A), indicating loss of crystallinity, but the crystallographic structure of the cubosomes remain the same. In PBS medium (Fig. 2-B), all the six peaks are still visible after lyophilization. (For interpretation of the references to colour in this figure legend, the reader is referred to the Web version of this article.)

channel increased by 3% and in PBS buffer it increased by 1.7%. From this, it is possible to infer that lyophilization barely affects the structural parameters of the cubosomes.

Besides the observed shift to smaller *q* values, it is also evident some changes in the height of the first diffraction peak for both systems (Fig. 2A and B). It is important to mention that the height of the first peak, in this case, can be related to the nanoparticle concentration (fewer scattering particles lead to a smaller diffraction peak) [37–39] or due to the loss of PHY-Cub inner cubic structure [33,40]. Noteworthy, such effect was less pronounced in the system composed by PBS buffer, as compared to the system in ultrapure water (Fig. 2A and B). According to SAXS measurements, PBS buffer can effectively preserve the inner structure of the cubosomes, since after the rehydrating process the scattering curves are quite similar (Fig. 2B), which is not the case for the system in ultrapure water (Fig. 2A), where only two peaks are evident indicating a loss of crystallinity in the system, as well as the concentration of cubic particles. Indeed, we believe that the loss of cubosome crystallinity is due to the lyophilization process, i.e., as water is taken away from the nanoparticle. Actually, during this process, some inner cylinders from the cubosome structure may collapse (scrambling all the lipids) in such a way that they are not able to return to its original arrangement after rehydration. Moreover, we cannot exclude the possibility of an entire cubosome collapsing during this process. Actually, this might be the case, according to our NTA data, where we evidenced a significant decrease in cubosome concentration. This concentration loss was also assessed by NTA as it will be shown latter in the text.

In literature there are not many details about the effect of lyophilization/freeze drying in the internal structure of the cubosomal nanoparticles. In 2017, Shi et al. produced both GMO and PHY cubosomes submitting them to a freeze drying processes, with the use of a cryoprotectant (manitol). The authors evidenced that the nanoparticles structure remained unaltered after this process. Interestingly, the authors also investigated the effect of a small diterpenoid named oridonin in the cubosomes inner symmetry. They observed that the drug was not able to change the nanoparticle crystallographic symmetry [15].

The influence of the lyophilization process on the cubosomes morphology and inner organization was evaluated by conventional TEM and cryo-EM. Fig. 3 shows a typical Cryo-EM micrograph of PHY-Cub, in ultrapure water, before undergoing any process (*control*). Image shows different nanoparticles sizes, ranging from 100 nm to 400 nm, whereas shapes can be either squared and rounded (see the arrows in Fig. 3).

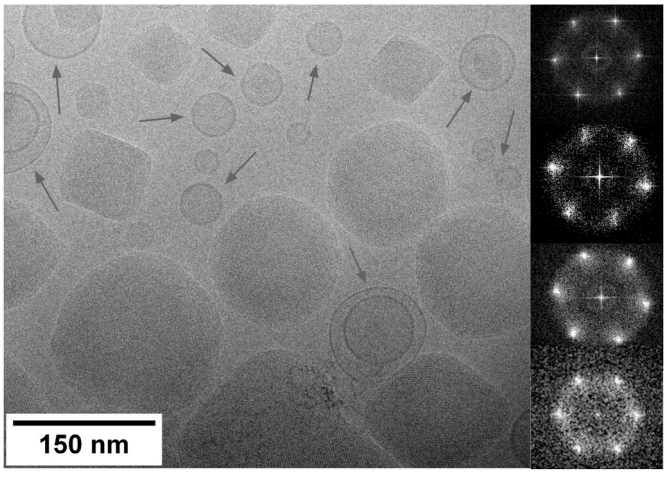

Fig. 3. Electron micrographs for PHY-Cub in the ultrapure water before undergoing any process (*control samples*). The arrows indicate the presence of vesicles coexisting with the cubosomes. The inset shows FFTs taken out of individual particles in the cryo-EM micrographs evidencing internal crystallographic inner structure. Particles with varied size and shape were observed, with sizes ranging from 100 nm to 400 nm.

Micrographs also revealed the presence uni- and multi-lamellar vesicles in the sample coexisting with PHY-cubs (see arrows in Fig. 3). These results are in good agreement with Akhlaghi et al. [33], where they also report presence of vesicles in the samples and particles in varied sizes from 50 nm to 300 nm [33], as well as others researchers [41,42]. Some examples of both monoolein and PHY-cubs presenting variable size and the presence of small liposomes can be found elsewhere [5,43]. In order to get more information on the PHY-Cub inner structure of each individual particle, we applied the FFT analysis. Fig. 3 also displays the FFT patterns for some of the PHY-Cub (right panel). Only particles with a clear FFT shape were taken into account for the lattice parameter calculation. The calculated lattices revealed a mean size of 6.7 ± 0.2 nm, compatible with the lattice parameters found by SAXS measurements. This analysis revealed individual cubosomes with varied lattice parameter ranging from 6.0 nm to 7.5 nm. Knowing that cubosomes could present both square and round shapes guided the measurements of conventional TEM for studying lyophilized samples.

TEM micrographs (Supplementary Fig. S1) revealed PHY-Cubs (control sample) structures, depicted nearly spherical cubosomes with irregular polyangular shapes. Most particles present sizes larger than 300 nm but smaller than 600 nm for the control sample, compatible with cryo-EM measurements (Fig. 3). Due to staining, there is no internal structure visible in the nanoparticles, only outer shapes. Supplementary Fig. S2 displays TEM micrographs of rehydrated lyophilized cubosomes in water, revealing particle diameters smaller than 500 nm. Before (*control*) or after the rehydrated lyophilized, there is no change in the outer shape of the nanoparticles, nor an influence on particle size from the TEM point of view.

DLS was also used to calculate nanoparticles size distribution and polydispersion index, PDI. DLS data analysis presumes that the scattering particles are homogeneous spheres in solution [44,45]. Nevertheless, this is not the case for cubosomes, which may have not-spherical shapes. In this technique it is possible to use the self-correlation function to provide information of the PHY-Cub system. According to the DLS analysis (see Supplementary Table 1), PHY-Cub hydrodynamic diameter, D_H, was 237 ± 5 nm and 229 ± 1 nm, for the systems in ultrapure water and PBS buffer, respectively. The polydispersity index, PDI, were 0.052 ± 0.005 and 0.056 ± 0.005, for systems in ultrapure water and PBS buffer, respectively, indicating very low polydispersion of sizes. Interestingly, in PBS buffer, it was observed a slightly smaller D_H PHY-Cub, as compared to the systems in ultrapure water. Both systems presented a nice monodispersity (PDI values < 0.1) [45].

After lyophilization and sample's rehydration in ultrapure water, nanoparticles presented *DH* and PDI of 229 ± 4 nm and 0.129 ± 0.005, respectively. For PBS buffer cubosomes the *DH* and PDI were 266 ± 3 and 0.207 ± 0.058, respectively. Curiously, *DH* of PHY-cubs in water presented a slight decrease (3.5%) in size but an increase (148%) in polydispersion. A more pronounced effect was observed for cubosomes in PBS, with an increase of 16% in size and 270% in polydispersion. Shi et al. did not mention the effect of freeze drying in the cubosomes size distribution [15]. This change in polydispersion can be expected once the original structure of the cubosomes was broken in some of the particles by the removal of the water content during lyophilization process. Rehydration can induce particles to be formed with a broader size distribution once water will be interacting with solid pieces of the bulk phase, in contrast with the already solubilized lipid in the bottom up sample preparation protocol [46].

In addition, we hypothesize that the presence of PBS ions on the solution (137 mM *NaCl*, 2.7 mM KCl, 8 mM Na_2HPO_4, and 2 mM KH_2PO_4, pH 7,4) can influence this breaking/conservation of nanoparticles. Indeed, we performed some measurements using HEPES buffer (10 mM, pH 7.4, data not shown) instead of PBS. Interestingly, we observed the same effect, i.e., a great impact in cubosome size as compared to ultrapure water. We, thus, believe that the ionic strength is not relevant in this process, but the presence of salt is more important. Somehow, the presence of salts can influence cubosomes particle size.

Nanoparticle Tracking Analysis (NTA) is a light scattering technique, also based on the Brownian motion, being able to detect particles sizes ranging from 10 up to 1000 nm [31,47,48]. This methodology allows one to obtain both the mean size distribution (similar to DLS) as well as scattering particle concentration [49,50]. In ultrapure water, PHY-Cub presented a mean size distribution of 166 ± 6 nm and the total particle concentration of (4.09 ± 0.66) x 10^{12} particles/mL before lyophilization (*control*). In PBS buffer, on the other hand, these values were 189 ± 4 nm and (6.67 ± 0.30) x 10^{12} particles/mL before lyophilization (*control*). Results displayed smaller *DH* sized than DLS measurements (see Supplementary Table 1). The discrepancy observed between the mean average size distribution and the hydrodynamic effective diameter can be related to the differences of the detection of the scattering light by each technique. DLS measurements are based on the light scattering fluctuation induced by the nanoparticles that are coming into and getting out the illuminated volume inside the cuvette. Thus it is a measurement of several scattering particles at the same time (herein, according to our data, the DLS concentration should be on the order of $10^{11} particles/mL$), whereas on NTA measures nanoparticle movement across a laser beam, using a quite diluted system ($\sim 10^{7} particles/mL$) and special cameras to get this movement [31,51,52]. In literature, is not common to find NTA measurements of cubosomes, a study by Azmi, Moghimi, and Yaghmur characterized PHY-cub using a sonication protocol, reporting particle mean size of 157 ± 22 nm with no mention about particle concentration or comparisons with DLS measurements [11]. In a more recent study, Prajapati, Larsen, and Yaghmur prepared GMO cubosomes, in PBS buffer, using a sonication method, revealing size distribution of 106 nm–131 nm, mentioning that dilution was prepared such as the particle concentration ranged between 10^{8} and 10^{9} particles/mL [53].

After the lyophilization process, PHY-cubs revealed a particle mean hydrodynamic size of 171 ± 6 nm for ultrapure water, evidencing that from the NTA point of view, the freeze drying process does not alter particle size. On the other hand, for PBS buffer, the observed value was 168 ± 9 nm, an increase of 16% after the lyophilization process, in very good agreement to the DLS data. Thus, we again attribute this effect due to the salt molecules in the buffer as compared to ultrapure water. Regarding total particle concentration, it was observed a value of (1.76 ± 0.47) x 10^{12} particles/mL in ultrapure water and (1.23 ± 0.19) x 10^{12} particles/mL in PBS buffer. As evidenced by SAXS, NTA confirms the decrease in particle concentration after the lyophilization process. Further evaluating particle size distribution (Supplementary Fig. S3 and Supplementary Fig. S4), it is clear that before the lyophilization process, control samples (in both water and PBS buffer) present less size populations than after the freeze-drying process. Which can be related to the lower polydispersion when the cubosomes are produced and a larger polydispersion when they are rehydrated from the lyophilization process, as evidenced by DLS. In addition, it is clear that particle concentration is smaller for lyophilized samples than in control samples, as evidenced by the different y-axis scales. Such comparison study was not found in literature up to this date regarding cubosomes.

3.2. Extrusion evidences cubosomes high degree of malleability

Cubosomes were submitted to extrusion process in order to investigate the nanoparticle malleability and ability to be compressed and subsequently swollen. Extrusion is a well-known process used to control size distribution of liposomes [54–56] as well as the ability to change a multilamellar to a unilamellar vesicles [57–59]. Fig. 4 displays the SAXS curves of the systems in ultrapure water (Fig. 4A) and in PBS buffer (Fig. 4B) for the non-extruded samples (*control*, red curves) and for the extruded systems using 100 nm (blue curves) and 50 nm (green curves) filters. To do so, a home-built extruder, with a Peltier-based temperature control was developed and samples were extruded at 45 °C in 11 cycles. As it is shown in Fig. 4, for both studied systems, in ultrapure water and PBS buffer, the extrusion process does not change the inner cubic symmetry of PHY-Cub (*Pn3m*), neither the lattice parameter nor calculated water channel, remaining approximately 6.8 nm for all samples (*control* or extruded), as shown in Table 1. Nonetheless, the height of the first peak of PHY-Cub was kept unaltered during extrusion, indicating that there is no significant change in the concentration of the nanoparticles before and after the process.

Nilsson et al. produced PHY based cubosomes mixed with oleic acid using a sonication protocol, afterwards applying extrusion in pore sizes ranging from 800 nm to 100 nm, displaying in the SAXS curves an indexing to the *Pn3m* cubic structure, however there was no mention of a measurement before the extrusion process [32]. Apart from their work, to this date, it was not found in literature a comparison of cubosomes before and after the extrusion process in order to evaluate detailed morphology changes.

TEM micrographs were acquired for extruded (50 nm pore size filter) cubosomes in water medium (see Supplementary Fig. S5). One can see particles with a varied shape, both round and polyangular. Sizes are variable, but most particles revealed diameters around 350 nm. When comparing with the control samples, see Supplementary Fig. S1, extruded particles reveal a slightly smaller size distribution. Based on TEM data, it is not possible to evaluate if the extrusion has an influence on particle size or not, nonetheless, the particles outer shape is not changed by the extrusion process.

DLS and NTA were performed to further explore the influence of extrusion on nanoparticle dimensions and malleability for the systems in the ultrapure water and PBS buffer, using different pore size filters: 400 nm, 200 nm, 100 nm, 50 nm and 30 nm. Such measurements were performed on the same day as the sample preparation and extrusion. On this ground, Fig. 5 and Table S1 in supplementary material displays both DLS and NTA data for PHY-Cub particles in water and PBS buffer media. In the presence of water (Fig. 5A - blue bars), DLS measurements reveal that cubosomes do not have their hydrodynamic size (*DH*) altered when

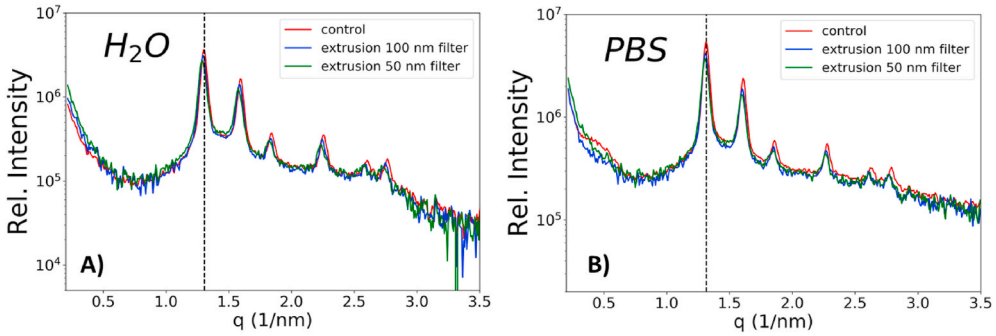

Fig. 4. SAXS curves of the systems in ultrapure water (A) and PBS buffer (B) for the non-extruded sample (*control*, red lines) and for the extruded systems using 100 nm (blue lines) and 50 nm (green lines) filters. For both systems, extrusion does not change the particles crystallographic group nor particle concentration. (For interpretation of the references to colour in this figure legend, the reader is referred to the Web version of this article.)

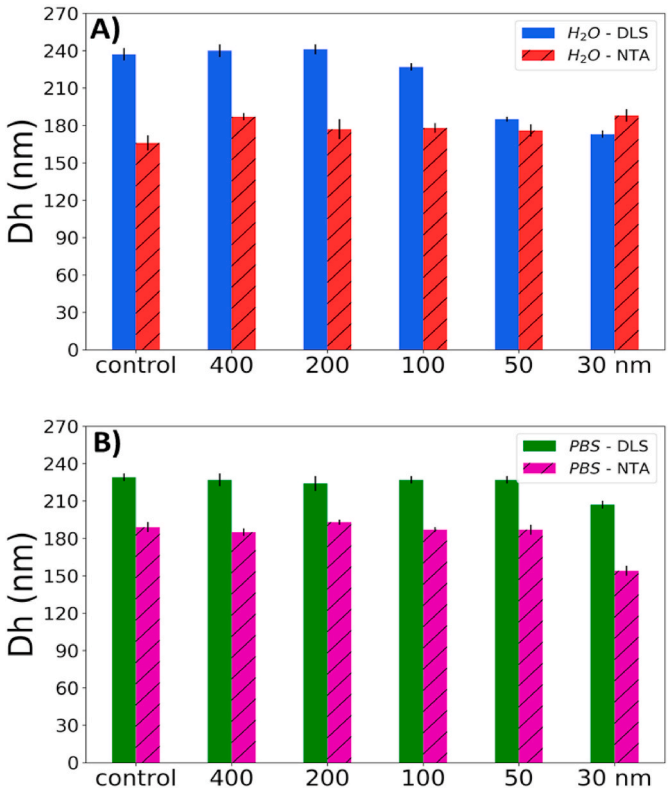

Fig. 5. DLS and NTA data for PHY-cub extruded in both (A) water and (B) PBS media. In one hand, for PHY-cub in water (A), DLS reveals that up to the 100 nm pore size, there is no significant difference in particle size, while for 50 nm and 30 nm pore sizes a decrease in particle size is visible. On the other hand, NTA data reveal no significant difference in particle size for all studied filters. For PHY-cub in PBS medium, a similar behavior is seen, DLS presents particles with compatible size up to the 50 nm filter and a decrease of particle size in the 30 nm filter. NTA data presents the same tendency. Overall, NTA data revealed smaller particles than DLS measurements.

extruded up to the 100 nm pore size filter. When extruded with 50 nm and 30 nm pore size filters, there is a decrease (~ 30%) in particle size. Such a fact is also confirmed by the autocorrelation functions as can be seen in Supplementary Fig. S6, where a slightly shift of the curves to smaller τ values are observed. The same behavior is observed in PBS medium (Fig. 5B - green bars) and Supplementary Fig. S7, but less pronounced as compared to the water medium. Comparing the aqueous media, PHY-Cub presented smaller *DH* in PBS medium than in water medium. On the other hand, NTA data revealed no significant change in *DH* for cubosomes in water or PBS buffer, only at the 30 nm pore size filter in PBS medium a decrease in particle size is seen, as evidenced in Fig. 5.

Comparing both DLS and NTA data, significant differences in *DH* are observed. As mentioned earlier in the text, this can be attributed to the differences in measurements between both techniques [51,52].

These results are in good agreement with those reported by Nilsson et al. where PHY-cubs were produced and samples were extruded with filter sizes ranging from 800 nm to 100 nm in order to make the size distribution narrower, for these cubosomes the final particles size and PDI were 158 ± 4 nm and 0.18 ± 0.02, respectively [32].

It is common practice to use extrusion in order to produce liposomes and unilamellar vesicles [55,56,60]. However, despite the method used - type of the extruder, number of cycles, velocity of extrusion, etc - one can always have a narrow size distribution for the liposomes, being similar to the pore size filter [58,61,62]. Curiously, PHY-Cub revealed a mean diameter quite larger than the pore size filter used in the extrusion, such a fact indicates that phytantriol cubosomes are rather malleable and flexible. No evidence of a broken membranes was found during the extrusion process. We hypothesize that cubosomes, when undergoing extrusion, are compressed into the pores and afterwards swollen back to their original shape and morphology. Even the applied pressure in the process does not seem to influence on breaking the inner cubic structure of the nanoparticles. Regarding polydispersion, data is shown in Supplementary Table S1 and Supplementary Fig. S8. In water medium, despite the fact that nominal values display an increasing trend, when evaluated within the uncertainties, one can see that there is no change in polydispersion of the samples throughout the extrusion process at all pore size filters studied. The same trend is observed for PBS buffer.

When evaluating particle concentration (Supplementary Table S1 and Supplementary Fig. S9), already in the first extrusion step (400 nm pore size) the concentration of particles is increased by 87% and 23% in water medium and PBS buffer, respectively. This can indicate that even though a mean particle size of ~ 200 nm was evidenced by DLS and NTA, the breaking of larger particles (>500 nm) present in the dispersion (evidenced by the arrows in Supplementary Fig. S10) into smaller ones increased the particle concentration. It is visible that before the extrusion (see Supplementary Fig. S10), there are some particles in the suspension with size larger than 450 nm (black arrow), but after the process, this population is no longer in the dispersion, and only particle with sizes smaller than 450 nm are present (red arrow). Such fact is well explained by the breaking of the larger particles into smaller ones, as the process of extrusion naturally does for liposomes for instance Ref. [56, 61]. This trend is more visible in the PBS buffer samples (see Supplementary Fig. S11), where before the extrusion, there are some particles in the suspension with size larger than 450 nm (black arrow), but after the process, this population is no longer detectable in the dispersion, and only particle with sizes smaller than ~ 360 nm are present (red arrow). The same behavior occurs in all studied pore size filters, as evidenced by the same analysis (data not shown). The only exception in this trend is a PBS sample extruded with the 30 nm pore size filter, where the concentration is kept unaltered when compared to the control sample. For this particular sample, it is thought that an actual filtering of bigger particles may happen, once the in the graphs there is no evident population of particles bigger than 400 nm, as evidenced in Supplementary Fig. S12. We hypothesize that this may be due to the salts in the PBS buffer making the cubosomes less malleable than in water medium. Nonetheless this analysis shown that even when going trough smaller pore sizes, the cubosomes have shown this ability to squeeze and swollen back to their original state. Up to this date no experimental or theoretical analysis was found in literature regarding cubosomes malleability. Such fact could be interesting in drug delivery nanoparticle preparation. It should be possible to load a drug into the cubosome during the swollen process.

4. Conclusion

Phytantriol (PHY) cubosomes were produced from a well-established protocol in both ultrapure water and PBS buffer. After lyophilization, it was found that cubosomes still hold their internal structure and morphology after rehydration. Regarding particle size, in one hand, DLS revealed a slight increase in nanoparticle size, *DH*. On the other hand, particle concentration is significantly decreased after the process, indicating a loss of cubic particles in the rehydration process. In order to investigate cubosomes malleability, the samples were submitted to extrusion over a number of pore size filters. It was found that cubosomes still hold their morphology after extrusion. In addition, DLS and NTA revealed that cubosomes are rather malleable nanoparticles, because they did not present a significant alteration of size, (*DH*), after the extrusion process even in the smallest pore size filters (30 nm). The polydispersion index was kept unaltered, according to DLS data. Nevertheless, concentration of particles increased (87% in water medium and 23% in PBS buffer) during the extrusion process, indicating that larger particles (>500 nm) were broken into smaller ones in the

process. We believe that this study can shed light in cubosome nanomechanical applications, in particular due to its high malleability, as evidenced herein. Perhaps this property can induce the use of cubosomes on other applications regarding nanotechnology.

CRediT authorship contribution statement

Barbara Malheiros: Conceptualization, Investigation, Formal analysis, Visualization, Writing - original draft. **Raphael Dias de Castro:** Writing - review & editing, Software, Formal analysis. **Mayra C.G. Lotierzo:** Writing - review & editing, Formal analysis. **Bruna R. Casadei:** Conceptualization, Supervision, Writing - review & editing. **Leandro R.S. Barbosa:** Conceptualization, Supervision, Writing - review & editing.

Declaration of competing interest

The authors declare that they have no known competing financial interests or personal relationships that could have appeared to influence the work reported in this paper.

Acknowledgement

Financial support for this research was provided by FAPESP (# 2015/15822-1), CAPES and CNPq (308692/2018-7, 420567/2016-0, 155970/2018-6). A special thanks to the National Laboratory of Synchrotron Light (LNLS), SAXS-1 beamline, and National Laboratory of Nanotechnology (LNNano), Campinas-SP, for the usage of their facilities. We thank also prof. Dr. Eneida de Paula and Ludmilla David from the Biomembranes Laboratory at the Institute of Biology, UNICAMP, Campinas-SP for helping with NTA measurements.

Appendix A. Supplementary data

Supplementary data to this article can be found online at https://doi.org/10.1016/j.jddst.2020.102149.

References

[1] Jiali Zhai, et al., Non-lamellar lyotropic liquid crystalline lipid nanoparticles for the next generation of nanomedicine, PMID: 31082192, ACS Nano 13 (6) (2019) 6178–6206, https://doi.org/10.1021/acsnano.8b07961. eprint:.
[2] P. Brendan, Dyett et al. "Fusion dynamics of cubosome nanocarriers with model cell membranes", Nat. Commun. 10 (1) (Oct. 2019) 4492.
[3] Zahra Karami, Mehrdad Hamidi, Cubosomes: remarkable drug delivery potential, Drug Discov. Today 21 (.5) (2016) 789–801.
[4] M. Jayne Lawrence, Surfactant systems: their use in drug delivery", Chem. Soc. Rev. 23 (6) (1994) 417–424.
[5] Patrick T. Spicer, et al., Novel process for producing cubic liquid crystalline nanoparticles (cubosomes), Langmuir 17 (19) (2001) 5748–5756, https://doi.org/10.1021/la010161w, eprint.
[6] Naga M. Lakshmi, et al., Cubosomes as targeted drug delivery systems - a biopharmaceutical approach, Curr. Drug Discov. Technol. 11 (3) (2014) 181–188.
[7] Haiqiao Wang, et al., Polymerization of cubosome and hexosome templates to produce complex microparticle shapes, J. Colloid Interface Sci. 546 (2019) 240–250.
[8] Elisabetta Esposito, et al., Structural studies of lipid based nanosystems for drug delivery: X-Ray Diffraction (XRD) and Cryogenic Transmission Electron Microscopy (cryo-TEM), 2015, pp. 861–889.
[9] Federica Carducci, et al., X-ray characterization of pharmaceutical and cosmetic lipidic nanoparticles for cutaneous application, Curr. Pharmaceut. Des. 25 (21) (2019) 2364–2374.
[10] Alexandre Lancelot, Teresa Sierra, José Luis Serrano, Nanostructured liquidcrystalline particles for drug delivery, Expet Opin. Drug Deliv. 11 (4) (2014) 547–564. PMID: 24490701.
[11] DM Azmi Intan, M Moghimi Seyed, Anan Yaghmur, Cubosomes and hexosomes as versatile platforms for drug delivery, Ther. Deliv. 6 (12) (2015) 1347–1364. PMID: 26652281.
[12] J. Mo, G. Milleret, M. Nagaraj, Liquid crystal nanoparticles for commercial drug delivery, Liquid Crystals Reviews 5 (2) (2017) 69–85.
[13] Vittorio Luzzati, et al., "Structure of the cubic phases of lipid–water systems", Nature 220 (5166) (Nov. 1968) 485–488.
[14] Maria Chountoulesi, et al., Cubic lyotropic liquid crystals as drug delivery carriers: physicochemical and morphological studies, Int. J. Pharm. 550 (1) (2018) 57–70.
[15] Xuan Shi, et al., Comparative studies on glycerol monooleate- and phytantriol-based cubosomes containing oridonin in vitro and in vivo, PMID: 26670780, Pharmaceut. Dev. Technol. 22 (3) (2017) 322–329, https://doi.org/10.3109/10837450.2015.1121496. eprint:.
[16] Hanna M.G. Barriga, Margaret N. Holme, Molly M. Stevens, "Cubosomes: the next generation of smart lipid nanoparticles?" In, Angew. Chem. Int. Ed. 58 (10) (2019) 2958–2978.
[17] Thiagarajan Madheswaran, et al., Current potential and challenges in the advances of liquid crystalline nanoparticles as drug delivery systems, Drug Discov. Today 24 (7) (2019) 1405–1412.
[18] Tri-Hung Nguyen, et al., Nanostructured liquid crystalline particles provide long duration sustained-release effect for a poorly water soluble drug after oral administration, J. Contr. Release 153 (2) (2011) 180–186.
[19] R. Nageshwar, Yepuri et al. "Deuterated phytantriol – a versatile compound for probing material distribution in liquid crystalline lipid phases using neutron scattering", J. Colloid Interface Sci. 534 (2019) 399–407.
[20] M El-Laithy Hanan, et al., Cubosomes as oral drug delivery systems: a promising approach for enhancing the release of clopidogrel bisulphate in the intestine, Chem. Pharm. Bull. (2018) c18, 00615.
[21] Hanan M. El-Laithy, et al., Stabilizing excipients for engineered clopidogrel bisulfate procubosome derived in situ cubosomes for enhanced intestinal dissolution: stability and bioavailability considerations, Eur. J. Pharmaceut. Sci. 136 (2019) 104954.
[22] Nazik A. Elgindy, Mohammed M. Mehanna, Salma M. Mohyeldin, Self-assembled nano-architecture liquid crystalline particles as a promising carrier for progesterone transdermal delivery, Int. J. Pharm. 501 (1) (2016) 167–179.
[23] Silvia Franzé, et al., Lyophilization of liposomal formulations: still necessary, still challenging, Pharmaceutics 10 (3) (2018) 139.
[24] Alex Langford, et al., Drying of biopharmaceuticals: recent developments, new technologies and future direction, Japan Journal of Food Engineering 19 (1) (2018) 15–24.
[25] Fonte Pedro, Salette Reis, Sarmento Bruno, Facts and evidences on the lyophilization of polymeric nanoparticles for drug delivery, J. Contr. Release 225 (2016) 75–86.
[26] Alberto A. Escobar-Puentes, et al., Preparation and characterization of succinylated nanoparticles from high-amylose starch via the extrusion process followed by ultrasonic energy, Food Bioprocess Technol. 12 (10) (2019) 1672–1682.
[27] Anna CNTF. Corrêa, et al., Liposomal taro lectin nanocapsules control human glioblastoma and mammary adenocarcinoma cell proliferation, Molecules 24 (3) (Jan. 2019).
[28] R. Vedanti, Salvi and Pravin Pawar. "Nanostructured lipid carriers (NLC) system: a novel drug targeting carrier", J. Drug Deliv. Sci. Technol. 51 (2019) 255–267.
[29] Mohammed Maniruzzaman, et al., A review of hot-melt extrusion: process technology to pharmaceutical products, International Scholarly Research Notices 2012 (2012).
[30] Peng Guo, et al., Nanomaterial preparation by extrusion through nanoporous membranes, Small 14 (18) (2018) 1703493.
[31] Lıgia Nunes de Morais Ribeiro, et al., Use of nanoparticle concentration as a tool to understand the structural properties of colloids, Sci. Rep. 8 (1) (2018) 1–8.
[32] Christa Nilsson, et al., SPECT/CT imaging of radiolabeled cubosomes and hexosomes for potential theranostic applications, Biomaterials 33 (34) (2013) 8491–8503.
[33] Seyedeh Parinaz Akhlaghi, et al., Impact of preparation method and variables on the internal structure, morphology, and presence of liposomes in phytantriol-Pluronic R F127 cubosomes, Colloids Surf. B Biointerfaces 145 (2016) 845–853.
[34] Raphael Dias de Castro, et al., SCryPTA: a web-based platform for analyzing Small-Angle Scattering curves of lyotropic liquid crystals, bioRxiv (2019), 791848, https://doi.org/10.1101/791848.
[35] Paolo Mariani, Vittorio Luzzati, Hervé Delacroix, Cubic phases of lipid-containing systems: structure analysis and biological implications, J. Mol. Biol. 204 (1) (1988) 165–189.
[36] Serena Mazzoni, et al., Cytochrome-c affects the monoolein polymorphism: consequences for stability and loading efficiency of drug delivery systems, Langmuir 32 (3) (2016) 873–881. PMID: 26710233.
[37] Diego G. Lamas, et al., 5 - X-ray diffraction and scattering by nanomaterials, in: L. Alessandra, Róz Da, et al. (Eds.), Micro and Nano Technologies, 2017, pp. 111–182.
[38] Michael Krumrey, Chapter 3.2.2 - small angle x-ray scattering (SAXS), in: Hodoroaba Vasile-Dan, E.S. Unger Wolfgang, G. Shard Alexander (Eds.), Micro and Nano Technologies, 2020, pp. 173–183.
[39] Kiselev Ma, et al., Analysis of the vesicular structure of nanoparticles in the phospholipid- based drug delivery system using SAXS data, Journal of Surface Investigation: X-ray, Synchrotron and Neutron Techniques 13 (1) (2019) 111–116.
[40] Marco Mendozza, et al., Inorganic nanoparticles modify the phase behavior and viscoelastic properties of non-lamellar lipid mesophases, J. Colloid Interface Sci. 541 (2019) 329–338.
[41] L. Sagalowicz, et al., Crystallography of dispersed liquid crystalline phases studied by cryo-transmission electron microscopy, J. Microsc. 221 (2) (2006) 110–121.
[42] Davide Demurtas, et al., Direct visualization of dispersed lipid bicontinuous cubic phases by cryo-electron tomography, Nat. Commun. 6 (1) (2015) 1–8.
[43] Laurent Sagalowicz, et al., Study of liquid crystal space groups using controlled tilting with cryogenic transmission electron microscopy, Langmuir 23 (24) (2007) 12003–12009.
[44] Benjamin Chu, Tianbo Liu, Characterization of nanoparticles by scattering techniques, J. Nanoparticle Res. 2 (1) (2000) 29–41.

[45] Jörg Stetefeld, Sean A. McKenna, R Patel Trushar, Dynamic light scattering: a practical guide and applications in biomedical sciences, Biophysical reviews 8 (4) (2016) 409–427.
[46] K Swarnakar Nitin, Thanki Kaushik, Sanyog Jain, Bicontinuous cubic liquid crystalline nanoparticles for oral delivery of doxorubicin: implications on bioavailability, therapeutic efficacy, and cardiotoxicity, Pharmaceut. Res. 31 (5) (2014) 1219–1238.
[47] Fanny Varenne, et al., Multimodal dispersion of nanoparticles: a comprehensive evaluation of size distribution with 9 size measurement methods, Pharmaceut. Res. 33 (5) (2016) 1220–1234.
[48] Maciej Jarzebski, et al., Particle tracking analysis in food and hydrocolloids investigations, Food Hydrocolloids 68 (2017) 90–101, 30th anniversary special issue.
[49] Vikram Kestens, et al., Validation of a particle tracking analysis method for the size determination of nano-and microparticles, J. Nanoparticle Res. 19 (8) (2017) 271.
[50] Kamyar Mehrabi, et al., Improvements in nanoparticle tracking analysis to measure particle aggregation and mass distribution: a case study on engineered nanomaterial stability in incineration landfill leachates, Environ. Sci. Technol. 51 (10) (2017) 5611–5621.
[51] Jun Hou, et al., Nanoparticle tracking analysis versus dynamic light scattering: case study on the effect of Ca2+ and alginate on the aggregation of cerium oxide nanoparticles, J. Hazard Mater. 360 (2018) 319–328.
[52] Kate P.M. McComiskey, Lidia Tajber, Comparison of particle size methodology and assessment of nanoparticle tracking analysis (NTA) as a tool for live monitoring of crystallisation pathways, Eur. J. Pharm. Biopharm. 130 (2018) 314–326.
[53] Rama Prajapati, SusanWeng Larsen, Anan Yaghmur, "Citrem–phosphatidylcholine nano-self-assemblies: solubilization of bupivacaine and its role in triggering a colloidal transition from vesicles to cubosomes and hexosomes", Phys. Chem. Chem. Phys. 21 (27) (2019) 15142–15150.
[54] Askell Hinna, et al., Filter-extruded liposomes revisited: a study into size distributions and morphologies in relation to lipid-composition and process parameters, J. Liposome Res. 26 (1) (2016) 11–20. PMID: 25826203.
[55] Sandy Gim Ming Ong, et al., Evaluation of extrusion technique for nanosizing liposomes, Pharmaceutics 8 (4) (2016) 36.
[56] N. Berger, et al., Filter extrusion of liposomes using different devices: comparison of liposome size, encapsulation efficiency, and process characteristics, Int. J. Pharm. 223 (1) (2001) 55–68.
[57] Suzana Šegota, Durdica Težak, Spontaneous formation of vesicles, Adv. Colloid Interface Sci. 121 (1) (2006) 51–75.
[58] P. Yogita, Patil and sameer jadhav. "Novel methods for liposome preparation", Chem. Phys. Lipids 177 (2014) 8–18.
[59] H. Jousma, et al., Characterization of liposomes. The influence of extrusion of multilamellar vesicles through polycarbonate membranes on particle size, particle size distribution and number of bilayers, Int. J. Pharm. 35 (3) (1987) 263–274.
[60] Li Tang, et al., Controlling the size and shape of liposomal ciprofloxacin nanocrystals by varying the lipid bilayer composition and drug to lipid ratio, J. Colloid Interface Sci. 555 (2019) 361–372.
[61] Junmin Zhu, et al., Surface modification of liposomes by saccharides: vesicle size and stability of lactosyl liposomes studied by photon correlation spectroscopy, J. Colloid Interface Sci. 289 (2) (2005) 542–550.
[62] Yechezkel Barenholz, et al., Influence of lipid composition on the thermotropic behavior and size distribution of mixed cationic liposomes, J. Colloid Interface Sci. 356 (1) (2011) 46–53.